JACS
JOURNAL OF THE AMERICAN CHEMICAL SOCIETY

Communication

pubs.acs.org/JACS

Adaptive Pores: Charge Transfer Modules as Supramolecular Handles for Reversible Pore Engineering of Mesoporous Silica

B. V. V. S. Pavan Kumar,[†] K. Venkata Rao,[‡] T. Soumya,[†] Subi J. George,*[,‡] and M. Eswaramoorthy*[,†]

[†]Nanomaterials and Catalysis Lab, Chemistry and Physics of Materials Unit, and [‡]Supramolecular Chemistry Laboratory, New Chemistry Unit, Jawaharlal Nehru Centre for Advanced Scientific Research, Jakkur P.O., Bangalore 560064, India

Supporting Information

ABSTRACT: We introduce a non-covalent pore engineering approach to achieve exceptional reversibility of functionalization in SBA-15 through viologen−pyranine charge transfer (CT) modules. By employing alkyl derivatives of pyranine as donors, we could exploit the strong CT interactions between pyranine and viologen to reversibly modify the pore size and philicity. The fast binding of the donors enables quick and facile functionalization within minutes at room temperature. The modularity of the approach enables modification of pores with custom-designed compositions, components, and functions. The high selectivity exhibited by viologen on the pore wall facilitated its use in a CT affinity column.

Functionalized mesoporous silicas have generated a great deal of attention by virtue of their enormous applications in catalysis,[1] adsorption,[2] drug delivery,[3] sensing,[4] and separation.[5] Pore engineering is of paramount importance in realizing many of their applications in the frontier areas and has been usually done by the covalent route.[6] However, the rigid covalently linked functional moieties often modify the pores irreversibly and give no room for further maneuverability with custom-designed functionality. One way to overcome this problem in covalent functionalization is to attach active functionalities[7] capable of responding to external stimuli such as light and pH to control the pore size and philicity (for modulation of molecular transport and shuttle-mediated catalysis). Integrating the covalent strategy with non-covalent functional modules[8] (supramolecular handles) is expected to offer high flexibility to the system because of their reversible nature.[9] The introduction of non-covalent functional modules within the nanopores of mesoporous silica would allow facile postsynthetic control over the pore size, adsorption, and transport properties.

As a proof of concept, we used non-covalent charge transfer (CT) interactions[10] between donor and acceptor molecules as a means to reversibly modify the nature of the pores of mesoporous silica SBA-15[11] (SBA). Viologen, an electron acceptor, was first directly linked to the pore walls of SBA through silane chemistry. By employing pyranine and its hexyl (PC_6)- and dodecyl (PC_{12})-substituted derivatives as donors, we were then able to demonstrate changes in the pore size and philicity of the functionalized mesoporous silica (Figure 1). Remarkable reversibility was also demonstrated by removal of the donor molecules by breaking the CT interactions through the reduction of viologen. To our knowledge, this is the first report of a modular approach to reversibly modify the pore size and philicity of mesoporous silica to a large extent. The modified pores showed selectivity for hydrophilic and hydrophobic macromolecules depending upon the philicity of the pores.

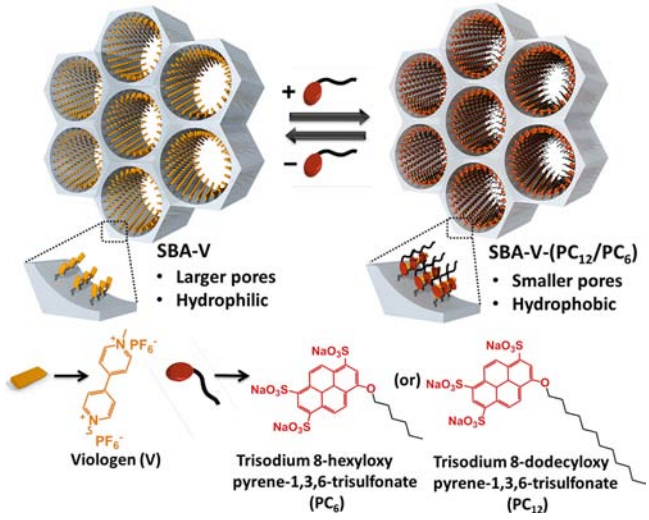

Figure 1. Concept of adaptive pores based on non-covalent CT modules. The viologen-modified mesopores of SBA-15 covalently functionalized with viologen (SBA-V) are non-covalently functionalized with hexyl (PC_6) and dodecyl (PC_{12}) derivatives of pyranine to reversibly vary the pore size and philicity. Reduction of the viologen moieties breaks the CT interactions between pyranine and viologen, enabling re-engineering of the pore.

Short SBA rods (1−2 μm) [Figure S1 in the Supporting Information (SI)] were synthesized following a reported procedure.[12] The pores were functionalized with (3-iodopropyl)trimethoxysilane using a surface polymerization approach.[6] The iodopropylsilane-modified SBA (SBA-I) was then reacted with excess *N*-methyl-4,4′-bipyridinium iodide to form SBA with covalently linked viologen moieties on the pore walls (SBA-V) (Figure S2). X-ray diffraction (XRD) patterns of SBA and SBA-V showed that the hexagonal structure of SBA was retained all through the functionalization steps (Figures S3a and S4). The N_2 adsorption isotherms of SBA, SBA-I, and SBA-V recorded at 77 K (Figure S3b) were of type IV according to the IUPAC classification[13] and characteristic of mesoporous materials with a narrow pore size distribution.[14] The pore size

Received: April 9, 2013
Published: July 17, 2013

dx.doi.org/10.1021/ja4035472 | *J. Am. Chem. Soc.* 2013, 135, 10902−10905

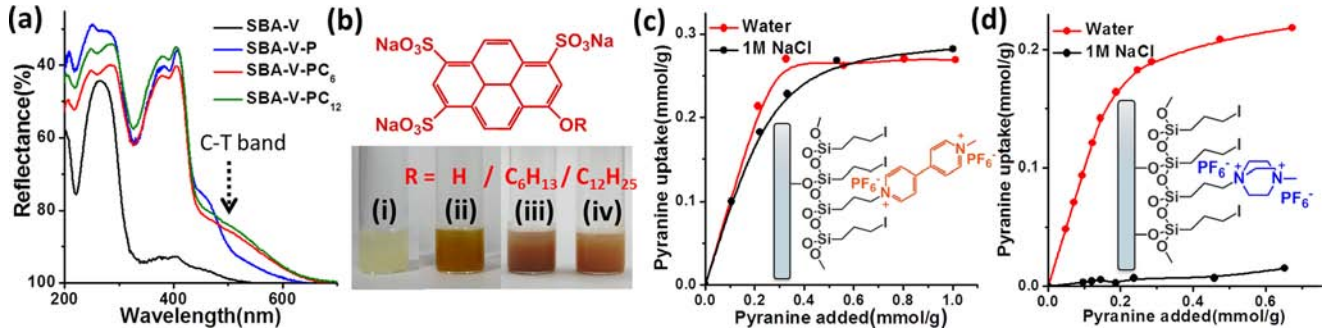

Figure 2. (a) UV−vis diffuse-reflectance spectra of SBA-V, SBA-V-P, SBA-V-PC_6, and SBA-V-PC_{12}, showing a CT band at 450−600 nm. (b) (top) General structure of pyranine (P) and its derivatives: R = H (P), C_6H_{13} (PC_6), and $C_{12}H_{25}$ (PC_{12}). (bottom) Photograph of dispersions of (i) SBA-V, (ii) SBA-V-P, (iii) SBA-V-PC_6, and (iv) SBA-V-PC_{12} in water (10 mg/mL). (c, d) Pyranine binding curves of (c) SBA-V and (d) SBA-B in water and 1 M NaCl solution. The insets show schematic representations of the pore walls of SBA-V and SBA-B, respectively.

distributions calculated using the Barrett−Joyner−Halenda (BJH) method[15] revealed a shift of average pore size from 10.3 nm for SBA to 8.3 nm for SBA-I (Figure S3b). Functionalization with viologen further reduced the pore size to 8.0 nm (Table ST1 in the SI). The small decrease in comparison with its large molecular dimensions (~0.9 nm) suggests that the viologen moieties may be placed in a tilted orientation inside the pores, although more conclusive evidence is needed to confirm this.

The amount of iodopropyl functional groups within SBA-I estimated from thermogravimetric analysis was ~1.8 mmol/g (Figure S5). The amount of viologen estimated from digestive analysis of SBA-V samples was found to be ~0.6 mmol/g (Figure S6), which is substantial enough to influence the pore properties.

The UV−vis diffuse-reflectance spectrum of SBA-V showed an intense peak at 265 nm corresponding to the aromatic $\pi \rightarrow \pi^*$ transition in the pyridinium rings (Figure 2a). Addition of pyranine (P) to SBA-V gave a distinct CT band at 450−600 nm (Figures 2a and S7) and an intense coloration of the resulting SBA-V-P hybrid, providing visual confirmation of the formation of CT complexes between viologen moieties and pyranine (Figures 2b and S8). Furthermore, binding titrations of SBA-V with pyranine revealed strong binding behavior, with an enhancement of an order of magnitude in the Langmuir binding constant (K_b) for viologen confined to the pores (1.4×10^5 M^{-1}; Figure S9) relative to the solution-state binding constant obtained by titrating pyranine with methyl viologen[16] (K_b = 1×10^4 M^{-1}). The difference in binding affinities was further evidenced by the complete uptake of pyranine by SBA-V from preassociated pyranine−methyl viologen CT complexes in solution (Figure S10). The binding curve, plotted as mmol of pyranine uptake versus mmol of pyranine added per gram of SBA-V (Figure 2c), shows an initial strong uptake up to 0.27 mmol/g followed by immediate saturation, usually associated with strong receptor-mediated binding. A kinetic study of the binding revealed that 98% of the binding was complete within 2 min of addition of pyranine to predispersed SBA-V (Figure S11). The steep pyranine uptake by SBA-V can be attributed to both CT interactions and the electrostatic interactions resulting from the dicationic viologen moieties. To understand the extent of the contribution from electrostatic interactions, an ionic hybrid control, SBA-B, was prepared by the reaction of SBA-I with 1,4-diazabicyclo[2.2.2]octane (DABCO) (Figure S2) and then subsequently reacted with excess CH_3I to form a dicationic ammonium salt on the pore wall. The binding titration of SBA-B with pyranine (Figures 2d and S8) showed uptake to 0.2 mmol/g and a gradual saturation, indicating weaker binding. These observations suggest that the electrostatic forces between viologen and pyranine also aid in the uptake for SBA-V. However, when the binding titration was carried out in 1 M NaCl solution, SBA-B showed negligible pyranine uptake (Figure 2d) because of screening of the electrostatic forces in the high-ionic-strength medium. On the other hand, SBA-V did not show any appreciable decrease in uptake in 1 M NaCl solution (Figure 2c). K_b decreased by only an order of magnitude in 1 M NaCl solution (1.4×10^4 M^{-1}; Figure S9), indicating a significant contribution from CT interactions in the uptake of pyranine.

The strong CT interactions between the hybrid viologen scaffold and pyranine were used to reversibly modify the pore size and philicity. The pyranine derivatives PC_6 and PC_{12} were used as donors for non-covalent functionalization of SBA-V. The viologen moieties on the pore walls efficiently complexed with PC_6 and PC_{12} to form colored complexes and give CT bands, just as in the case of pyranine (Figures 2a,b and S12). The N_2 adsorption isotherms of SBA-V containing non-covalently functionalized pyranine derivatives retained the type-IV behavior (Figure S13). However, the spinodal condensation transition shifted to lower P/P_o, implying constriction of the pore size, which was reduced from 8.0 nm for SBA-V to 6.7 nm for SBA-V-PC_6 and 6.0 nm for SBA-V-PC_{12} (Figure 3 and Table ST1), in conformance with the alkyl chain lengths. The pore size

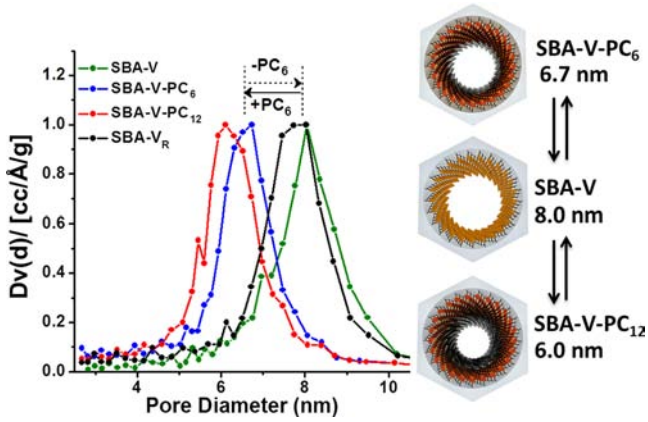

Figure 3. Normalized BJH pore size distributions of SBA-V, SBA-V-PC_6, and SBA-V-PC_{12} showing the decrease in pore size upon addition of PC_6 or PC_{12}. The reversal of pore size upon removal of PC_6 is indicated by the dotted arrow. The schematic on the right (not to scale) illustrates the decrease in pore size upon functionalization with PC_6 and PC_{12}.

dx.doi.org/10.1021/ja4035472 | J. Am. Chem. Soc. 2013, 135, 10902−10905

distributions for SBA-V-PC_6 and SBA-V-PC_{12} had full widths at half-maximum (fwhm) similar to that of SBA-V, indicating uniform supramolecular functionalization (Figure 3). The pyranine derivatives could be removed by breaking the CT interactions through reduction of viologen followed by washing with salt solution and oxidation using O_2, giving SBA-V_R. Remarkably, the removal of PC_6 restored the pore size to 8.0 nm, and further addition of PC_6 again reduced the pore size to ~7 nm. The incomplete reversal of pore size upon addition of PC_6 was probably due to the degradation of some viologen moieties during oxidation through the superoxide mechanism.[17] This degradation was overcome by the use of a milder oxidizing agent, $K_3[Fe(CN)_6]$, which enabled reversible pore switching for up to three cycles (Figure S14).

Non-covalent attachment of pyranine derivatives to SBA-V modified not only the pore size but also the philicity because of the presence of the hydrophobic alkyl chains. Water sorption isotherms were recorded to follow the change in philicity of the pores[18] (Figure 4a,b). Functionalization of SBA with viologen

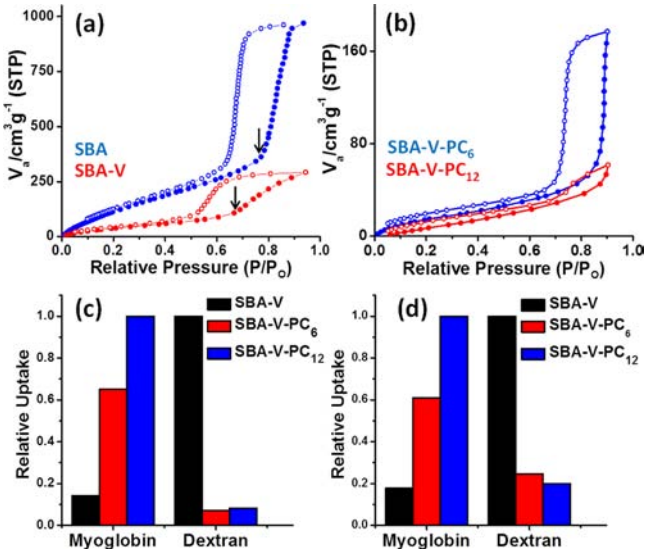

Figure 4. (a, b) Water sorption isotherms of (a) SBA and SBA-V and (b) SBA-V-PC_6 and SBA-V-PC_{12} recorded at 298 K. (c, d) Relative uptakes of myoglobin and FITC-dextran (4 kDa) by SBA-V, SBA-V-PC_6, and SBA-V-PC_{12} in (c) individual and (d) mixed adsorption experiments, showing philicity-driven uptake.

shifted the pore-filling transition of SBA from $P/P_o \approx 0.8$ to $P/P_o \approx 0.7$. Complexation of these viologen moieties with PC_6 shifted the pore condensation to higher P/P_o (~0.85). It should be noted that there was a concomitant decrease in pore size as well, which would shift the pore-filling transition to lower P/P_o; therefore, the increase in hydrophobicity is greater than what is apparent from the shift of the transition from 0.7 to 0.85. This change was more prominent for SBA-V-PC_{12}, which showed very poor uptake of water. The values of the Brunauer–Emmett–Teller (BET) constant "C" derived from the N_2 adsorption isotherms for SBA-V containing pyranine derivatives are small, indicating low heats of adsorption, in good agreement with the water sorption behavior[19] (Table ST1).

This variation in the philicity among SBA-V, SBA-V-PC_6, and SBA-V-PC_{12} was further demonstrated by their selective uptakes of hydrophilic fluorescein isothiocyanate (FITC)-labeled dextran and the hydrophobic protein myoglobin. The adsorption of protein was carried out at its isoelectric pH (7.2) to avoid any influence of pore surface charge. The molecular dimensions of myoglobin and 4 kDa dextran are 2.9 nm × 3.6 nm × 6.4 nm and 3 nm, respectively. SBA-V-PC_{12} and SBA-V-PC_6 exhibited stronger uptake of myoglobin relative to dextran (hydrophilic), indicating hydrophobicity-driven uptake. However, SBA-V showed a higher uptake of dextran relative to myoglobin, implying hydrophilicity-driven uptake (Figure 4c). The same trend was also observed in the mixed adsorption study, where dextran and myoglobin were added together (Figure 4d). It is noteworthy that SBA covalently linked with hexyl chains (SBA-C_6) exhibited 2 times lesser myoglobin uptake than SBA-V-PC_6 (Figure S15).

We also examined the selectivity of SBA-V for two different donors, coronene tetracarboxylate (CS) and perylene tetracarboxylate (PS), which bear similar molecular charge but differ in their CT interaction strength (Figure S16). Methyl viologen showed a selectivity factor of 1.2 for CS over PS (Figure S17). On the other hand, SBA-V showed a selectivity factor of 45, representing a huge (38-fold) enhancement relative to the selectivity factor obtained for free methyl viologen in solution (Figure S18). This would enable highly efficient dip-based single-step separation of CS from mixtures of CS and PS. To check for separation in a flow-based system, breakthrough experiments[20] were performed on a bed of SBA-V using an equimolar mixture of CS and PS. As expected from the static binding selectivity, PS eluted faster through the column and was the first to break through in its pure form, followed by CS (Figure 5a). The

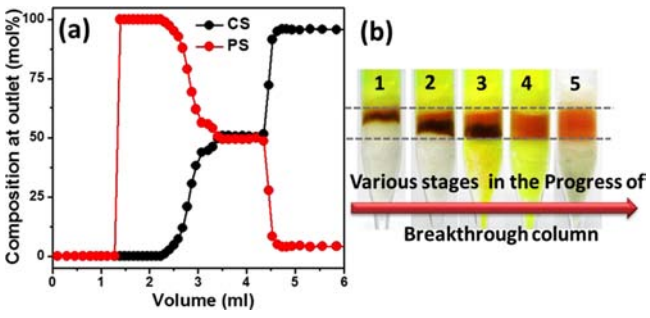

Figure 5. (a) Experimental breakthrough curves for an equimolar mixture of CS and PS flowing through a bed of SBA-V, exhibiting clear separation and high selectivity. (b) Photographs of the bed of SBA-V (located between the dashed lines) at various stages of the breakthrough experiment.

separation could be followed easily since CS and PS form CT complexes with different colors (orangish brown for CS and dark brown for PS). As the feed solution passed through, it separated into a faster-traveling pure PS band and a CS-rich band [Figure 5b(2–3)]. Gradually, all of the viologen moieties became saturated with CS, at which point the outlet composition reached equimolar [Figure 5b(4–5)]. A water purge was then applied to elute the adsorbed contents, and the outlet molar composition quickly stabilized at CS/PS = 96:4 (Figure 5a). The dynamic binding capacity of SBA-V was found to be ~35% of its static binding capacity, which is very significant because of the high retention of efficiency even in a flow-based system. We also obtained clear breakthrough curves for a three-component equimolar mixture of CS, PS, and pyrene tetrasulfonate, all of which have the same molecular charge but different CT properties (Figure S19). Thus, the viologen groups on the pore walls exhibit increased strength of binding coupled with

dx.doi.org/10.1021/ja4035472 | J. Am. Chem. Soc. 2013, 135, 10902–10905

enhanced selectivity and fast dynamics, making them ideal modules for non-covalent functionalization.

In conclusion, we have shown a novel non-covalent strategy for modular and reversible functionalization of mesopores using CT interactions. The adaptive nature of the pores in mesoporous silica was clearly demonstrated through N_2 and water sorption studies as well as selective uptake of macromolecules. The increased strength and fast dynamics of pyranine binding to viologen on the pore walls make them ideal modules for non-covalent modification of the pore size and philicity. The enhanced selectivity of SBA-V on the basis of CT interactions also enables facile separation of highly water-soluble donors that cannot be separated through conventional strategies. Incorporation of multiple functionalities into the mesopores through the conventional covalent silane pathway cannot be directly controlled because different silanes have varying hydrolysis rates in solution. The modularity of the approach enables modification of pores with custom-designed compositions, components, and functions. We envisage that this non-covalent methodology should enable uniform distribution of functional groups by virtue of its reversible nature. Furthermore, it is also conceivable that these non-covalent modules within the confines of the pores can be designed to undergo nonequilibrium and dynamic redistribution in response to external stimuli, akin to biological systems.[21]

■ ASSOCIATED CONTENT

Supporting Information

Experimental procedures, instrumentation details, and supporting figures and tables. This material is available free of charge via the Internet at http://pubs.acs.org.

■ AUTHOR INFORMATION

Corresponding Author

eswar@jncasr.ac.in; george@jncasr.ac.in.

Notes

The authors declare no competing financial interest.

■ ACKNOWLEDGMENTS

This work is dedicated to Prof. C. N. R. Rao, who is turning 80 this year. The authors thank A. Hazra and R. Haldar for water sorption measurements and M. Kumar and A. Jain for helpful discussions. For fellowships, B.V.V.S.P.K. and K.V.R. thank CSIR and T.S. thanks SRFP.

■ REFERENCES

(1) (a) Maschmeyer, T.; Rey, F.; Sankar, G.; Thomas, J. M. *Nature* **1995**, *378*, 159. (b) Corma, A. *Chem. Rev.* **1997**, *97*, 2373. (c) Choi, M.; Cho, H. S.; Srivastava, R.; Venkatesan, C.; Choi, D.-H.; Ryoo, R. *Nat. Mater.* **2006**, *5*, 718.

(2) (a) Kuwahara, Y.; Kang, D.-Y.; Copeland, J. R.; Brunelli, N. A.; Didas, S. A.; Bollini, P.; Sievers, C.; Kamegawa, T.; Yamashita, H.; Jones, C. W. *J. Am. Chem. Soc.* **2012**, *134*, 10757. (b) Walcarius, A.; Mercier, L. *J. Mater. Chem.* **2010**, *20*, 4478.

(3) (a) Vallet-Regí, M.; Balas, F.; Arcos, D. *Angew. Chem., Int. Ed.* **2007**, *46*, 7548. (b) Coll, C.; Bernardos, A.; Martínez-Máñez, R.; Sancenón, F. *Acc. Chem. Res.* **2013**, *46*, 339. (c) Vivero-Escoto, J. L.; Huxford-Phillips, R. C.; Lin, W. *Chem. Soc. Rev.* **2012**, *41*, 2673. (d) Ferris, D. P.; Zhao, Y. L.; Khashab, N. M.; Khatib, H. A.; Stoddart, J. F.; Zink, J. I. *J. Am. Chem. Soc.* **2009**, *131*, 1686.

(4) (a) Radu, D. R.; Lai, C.-Y.; Wiench, J. W.; Pruski, M.; Lin, V. S. Y. *J. Am. Chem. Soc.* **2004**, *126*, 1640. (b) Lin, V. S. Y.; Lai, C.-Y.; Huang, J.; Song, S.-A.; Xu, S. *J. Am. Chem. Soc.* **2001**, *123*, 11510.

(5) (a) Yamaguchi, A.; Teramae, N. *Anal. Sci.* **2008**, *24*, 25. (b) Ma, X.; Wang, X.; Song, C. *J. Am. Chem. Soc.* **2009**, *131*, 5777.

(6) (a) Inagaki, S.; Guan, S.; Ohsuna, T.; Terasaki, O. *Nature* **2002**, *416*, 304. (b) Feng, X. *Science* **1997**, *276*, 923. (c) Hoffmann, F.; Cornelius, M.; Morell, J.; Fröba, M. *Angew. Chem., Int. Ed.* **2006**, *45*, 3216. (d) Linares, N.; Serrano, E.; Rico, M.; Balu, A. M.; Losada, E.; Luque, R.; Garcia-Martinez, J. *Chem. Commun.* **2011**, *47*, 9024.

(7) (a) Liu, N.; Chen, Z.; Dunphy, D.; Jiang, Y.-B.; Assink, R.; Brinker, C. J. *Angew. Chem., Int. Ed.* **2003**, *42*, 1731. (b) Alvaro, M.; Ferrer, B.; Garcia, H.; Rey, F. *Chem. Commun.* **2002**, 2012. (c) Wang, H.; Yang, H.; Liu, H.; Yu, Y.; Xin, H. *Langmuir* **2013**, *29*, 6687.

(8) Aida, T.; Meijer, E. W.; Stupp, S. I. *Science* **2012**, *335*, 813.

(9) (a) Winter, A.; Hoeppener, S.; Newkome, G. R.; Schubert, U. S. *Adv. Mater.* **2011**, *23*, 3484. (b) Carter, T. G.; Yantasee, W.; Sangvanich, T.; Fryxell, G. E.; Johnson, D. W.; Addleman, R. S. *Chem. Commun.* **2008**, 5583.

(10) (a) Au-Yeung, H. Y.; Pantoş, G. D.; Sanders, J. K. M. *Proc. Natl. Acad. Sci. U.S.A.* **2009**, *106*, 10466. (b) Rauwald, U.; Scherman, O. A. *Angew. Chem., Int. Ed.* **2008**, *47*, 3950. (c) Shimomura, S.; Matsuda, R.; Tsujino, T.; Kawamura, T.; Kitagawa, S. *J. Am. Chem. Soc.* **2006**, *128*, 16416. (d) Okabe, A.; Fukushima, T.; Ariga, K.; Aida, T. *Angew. Chem.* **2002**, *114*, 3564. (e) Tian, F.; Jiao, D.; Biedermann, F.; Scherman, O. A. *Nat. Commun.* **2012**, *3*, 1207. (f) Rao, K. V.; Jayaramulu, K.; Maji, T. K.; George, S. J. *Angew. Chem., Int. Ed.* **2010**, *49*, 4218.

(11) Zhao, D.; Feng, J.; Huo, Q.; Melosh, N.; Fredrickson, G. H.; Chmelka, B. F.; Stucky, G. D. *Science* **1998**, *279*, 548.

(12) Sayari, A.; Han, B.-H.; Yang, Y. *J. Am. Chem. Soc.* **2004**, *126*, 14348.

(13) Sing, K. S. W.; Everett, D. H.; Haul, R. A. W.; Moscou, L.; Pierotti, R. A.; Rouquerol, J.; Siemieniewska, T. *Pure Appl. Chem.* **1985**, *57*, 603.

(14) Beck, J. S.; Vartuli, J. C.; Roth, W. J.; Leonowicz, M. E.; Kresge, C. T.; Schmitt, K. D.; Chu, C. T. W.; Olson, D. H.; Sheppard, E. W. *J. Am. Chem. Soc.* **1992**, *114*, 10834.

(15) Barrett, E. P.; Joyner, L. G.; Halenda, P. P. *J. Am. Chem. Soc.* **1951**, *73*, 373.

(16) de Borba, E. B.; Amaral, C. L. C.; Politi, M. J.; Villalobos, R.; Baptista, M. S. *Langmuir* **2000**, *16*, 5900.

(17) Tagliazucchi, M.; Amin, V. A.; Schneebeli, S. T.; Stoddart, J. F.; Weiss, E. A. *Adv. Mater.* **2012**, *24*, 3617.

(18) Kimura, T.; Suzuki, M.; Maeda, M.; Tomura, S. *Microporous Mesoporous Mater.* **2006**, *95*, 213.

(19) Osaheni, J. A.; Buddle, S. T. U.S. Patent 6,193,412 B1, 2001.

(20) Bloch, E. D.; Queen, W. L.; Krishna, R.; Zadrozny, J. M.; Brown, C. M.; Long, J. R. *Science* **2012**, *335*, 1606.

(21) Mann, S. *Nat. Mater.* **2009**, *8*, 781.